

LA-UR-03-5559

Approved for public release;  
distribution is unlimited.

*Title:* Gamma radiation induced background determination for  
(n,g) measurements with 4p detectors

*Author(s):* R. Reifarh, T.A. Bredeweg, J.C. Browne, E.I. Esch, R.C.  
Haight, J.M. O'Donnell, A. Kronenberg, R.S. Rundberg, J.L.  
Ullmann, D.J. Vieira, J.B. Wilhelmy, J.M. Wouters; LANL,  
USA  
U. Greife; Colorado School of Mines, Golden, Colorado,  
80401, USA

*Submitted to:* DANCE project



Los Alamos National Laboratory, an affirmative action/equal opportunity employer, is operated by the University of California for the U.S. Department of Energy under contract W-7405-ENG-36. By acceptance of this article, the publisher recognizes that the U.S. Government retains a nonexclusive, royalty-free license to publish or reproduce the published form of this contribution, or to allow others to do so, for U.S. Government purposes. Los Alamos National Laboratory requests that the publisher identify this article as work performed under the auspices of the U.S. Department of Energy. Los Alamos National Laboratory strongly supports academic freedom and a researcher's right to publish; as an institution, however, the Laboratory does not endorse the viewpoint of a publication or guarantee its technical correctness.

Form 836 (8/00)

# Gamma radiation induced background determination for (n, $\gamma$ ) measurements with $4\pi$ detectors

R. Reifarh<sup>a</sup>, T.A. Bredeweg<sup>a</sup>, J.C. Browne<sup>a</sup>, E.I. Esch<sup>a</sup>, U. Greife<sup>b</sup>, R.C. Haight<sup>a</sup>,  
J.M. O'Donnell<sup>a</sup>, A. Kronenberg<sup>a</sup>, R.S. Rundberg<sup>a</sup>, J.L. Ullmann<sup>a</sup>, D.J. Vieira<sup>a</sup>,  
J.B. Wilhelmy<sup>a</sup>, J.M. Wouters<sup>a</sup>

<sup>a</sup> *Los Alamos National Laboratory, Los Alamos, New Mexico, 87545, USA*

<sup>b</sup> *Colorado School of Mines, Golden, Colorado, 80401, USA*

## Table of contents

Table of contents .....	1
List of figures .....	1
List of tables .....	2
1 Introduction .....	3
2 Types of background .....	3
3 Determination of (n,n) and ( $\gamma$ ,X) background .....	6
3.1 Cross sections .....	6
3.2 Detector response .....	10
4 Conclusions .....	21
References .....	21

## List of figures

Figure 1: Total $\gamma$ -ray cross sections for different isotopes as a function of energy [5]. .....	5
Figure 2: Comparison of (n,X) and ( $\gamma$ ,X) cross sections for gold. ....	6
Figure 3: Photon activity measured at FP14 at april-17 2003, 3 month after the shut down of the accelerator. ....	7
Figure 4: Comparison of (n,X) and ( $\gamma$ ,X) cross sections for sulfur. ....	8
Figure 5: Comparison of (n,X) and ( $\gamma$ ,X) cross sections for titanium. ....	9
Figure 6: Comparison of (n,X) and ( $\gamma$ ,X) cross sections for lead. ....	9
Figure 7: Comparison of (n,X) and ( $\gamma$ ,X) cross sections for carbon. ....	10
Figure 8: Response of the BaF <sub>2</sub> -array to g-rays of different energies interacting with a sulfur sample (5 mm thickness) in the center of the detector. ....	11
Figure 9: Comparison S(n, $\gamma$ ) (black) S( $\gamma$ ,X) (blue) and S(n,X) (red). ....	12
Figure 10: Response of the BaF <sub>2</sub> -array to g-rays of different energies interacting with a gold sample (0.2 mm thickness) in the center of the detector. ....	13
Figure 11: Comparison Au(n, $\gamma$ ) (black) Au( $\gamma$ ,X) (blue) and Au(n,X) (red). ....	14
Figure 12: Response of the BaF <sub>2</sub> -array to g-rays of different energies interacting with a carbon sample (10 mm thickness) in the center of the detector. ....	15
Figure 13: Comparison C(n, $\gamma$ ) (black) C( $\gamma$ ,X) (blue) and C(n,X) (red). ....	16
Figure 14: Response of the BaF <sub>2</sub> -array to g-rays of different energies interacting with a lead sample (0.2 mm thickness) in the center of the detector. ....	17
Figure 15: Comparison Pb(n, $\gamma$ ) (black) Pb( $\gamma$ ,X) (blue) and Pb(n,X) (red). ....	18

Figure 16: Response of the BaF <sub>2</sub> -array to g-rays of different energies interacting with a beryllium sample (10 mm thickness) in the center of the detector. ....	19
Figure 17: Comparison Be(n,γ) (black) Be(γ,X) (blue) and Be(n,X) (red). ....	20

## List of tables

Table 1: Summary of the neutron scattering cross sections for keV-neutrons and total reaction cross section for 10 MeV γ-rays of different isotopes.....	6
--	---

# 1 Introduction

Neutron capture measurements at white neutron sources have been carried out for more than 30 years. Important improvements in the realm of detector development during the last years allow measurements with higher accuracy on targets of smaller masses. A recent review comparing the most important present-day experimental facilities has been made by P. Koehler [1].

There are two main principles producing neutrons over a broad energy range:

- Electron-LINAC: Facilities like ORELA at Oak Ridge National Laboratory [2] and GELINA Geel [3, 4] are producing electrons of several hundred MeV and bombard a high-Z target. High energy  $\gamma$ -rays, mainly produced via bremsstrahlung, then induce  $(\gamma, n)$ -reactions in the target material to produce neutrons.
- Spallation sources: At facilities like n-TOF CERN [5] and LANSCE Los Alamos [6] protons up to several GeV are directed to a high-Z target, where neutrons are produced by spallation reactions.

Both solutions generate not only a prompt  $\gamma$ -flash, but also a delayed  $\gamma$ -ray background, caused by capture of moderated neutrons, arriving at the sample position at the same time of flight as neutrons.

The DANCE (Detector for Advanced Neutron Capture Experiments) project at flight path 14 (FP14) at the Lujan Center at the Los Alamos National Laboratory is designed to measure neutron capture cross sections using very small ( $\sim$ mg) samples. The neutrons are produced via spallation reactions caused by a 800 MeV proton beam hitting a tungsten cylinder. FP14 is designed to view only an upper tier water moderator and not the tungsten target itself. The main focus of this report is to investigate possibilities to disentangle the target originating  $\gamma$ -background from background caused by scattered neutrons at the sample assuming a DANCE like detector to measure detect the capture events.

## 2 Types of background

Direct neutron capture measurements have to face 4 major types of background:

1. **Time-independent**, which is not correlated with the neutron beam. Natural radioactivity or, in case of  $\text{BaF}_2$  detectors, intrinsic radioactivity are prominent examples.
2. **Time-dependent**, is every background component, which is correlated with the time structure of the beam, but does **not** scale with the size of the **sample** in the beam. Examples are neutrons from other experiments, or any particles originating at the neutron production area.
3. Even though **sample related** background reactions show a time dependence, they are considered extra within this discussion. Too main components contribute to the sample related background:
  - a)  **$(n, n)$**  reactions, where the neutrons are eventually captured in the surrounding material (in case of DANCE mainly  $\text{BaF}_2$ ) and create a similar signature as capture in the sample.

- b) ( $\gamma X$ ), where X includes all the possible interaction mechanisms between matter and photons (photo-effect, Compton scattering, pair production etc.). Most of the interactions are with the electrons in the sample material.

While (1) and (2) are usually determined by simple beam on/off and sample in/out experiments, more sophisticated attempts are needed for the sample related background (3). In order to determine the background due to scattered neutron (3a) either the time structure or the energy information of the total  $\gamma$ -ray energy released is used. Classical (n, $\gamma$ ) experiments were optimized to have very low neutron sensitivity ( $C_6D_6$ ) and could only measure the resonant part of the cross section. All the events, which appeared at time of flight “between resonances” were considered to be background. The neutron scatter background was not measured, but believed to be negligible. However, as it turned out, this method works fine only if the capture to scatter cross section ratio is not too small and the uncertainties required are in the order of 10 %. For higher accuracies or less favorable cases it turned out to be more successful to determine the background by detecting all the  $\gamma$ -rays emitted during an event. Even though this means using detector material with higher neutron sensitivity, the advantage of being able to disentangle between neutron captures on different isotopes (sample, backing, environment) using e.g. the total energy released eventually allows much lower systematic uncertainties. Furthermore the significantly higher detection efficiency of such setups allows the use of smaller samples.

Background due to  $\gamma$ -rays (3b), which are produced at the neutron production site or along the beam line due to neutron capture reactions can arrive at the sample position at the same time of flights like the neutrons under investigation. Without a sample in the beam, these gammas would not be detected, but since they interact with the sample, mainly via Compton-scattering and pair production, secondary gammas will be detected. Obviously this background scales with the sample size. So far the only way to determine the background caused by interactions of these  $\gamma$ -rays with the sample is using so called black resonance filters or polyethylene. The black resonance method follows the idea of putting material between the sample and the neutron production target in the beam, which has strong, but ideally narrow resonances. The material needs to be thick enough that all the neutrons with the right (resonance) energy are absorbed or scattered, while the cross section for the photons remains flat Figure 1. Within the TOF-window of the resonance, only “background” will then be measured. Similarly hydrogen is known to have huge neutron scattering cross section and comparably small photon cross sections. Therefore a polyethylene sample would reduce the neutron flux much more than the  $\gamma$ -ray flux and estimates about the relative strength are possible. Both methods, however, suffers from two main problems. First the filter will also reduce the  $\gamma$ -ray background and second the filter will cause other background too, because the scattered neutrons will eventually be captured and therefore create another source of background.

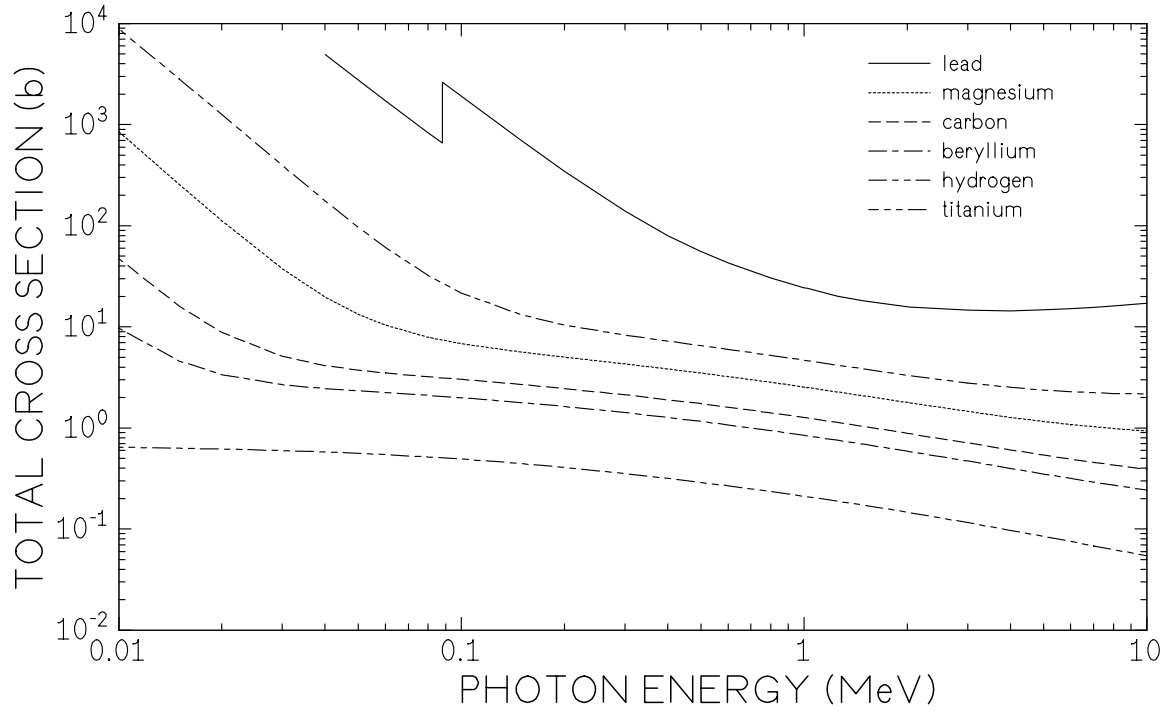


**Figure 1:** Total  $\gamma$ -ray cross sections for different isotopes as a function of energy [7].

Additionally, events due to scattered neutrons at earlier times might appear during this TOF-window, most of the neutrons will be – time consuming – moderated before the final capture. Disentangling between **(3a)** and **(3b)** is therefore a challenge for modern high accuracy (n, $\gamma$ ) experiments.

A first step to determine the background would be to measure the  $\gamma$ -ray spectrum at the sample position. Since neutron scattering and photon interaction cross sections with the sample are generally of the same order of magnitude (Figure 2), it is not obvious how to disentangle the two components. In the following chapter an attempt of determining the different components of the  $\gamma$ -ray background using certain isotopes in the beam at the sample position will be described.

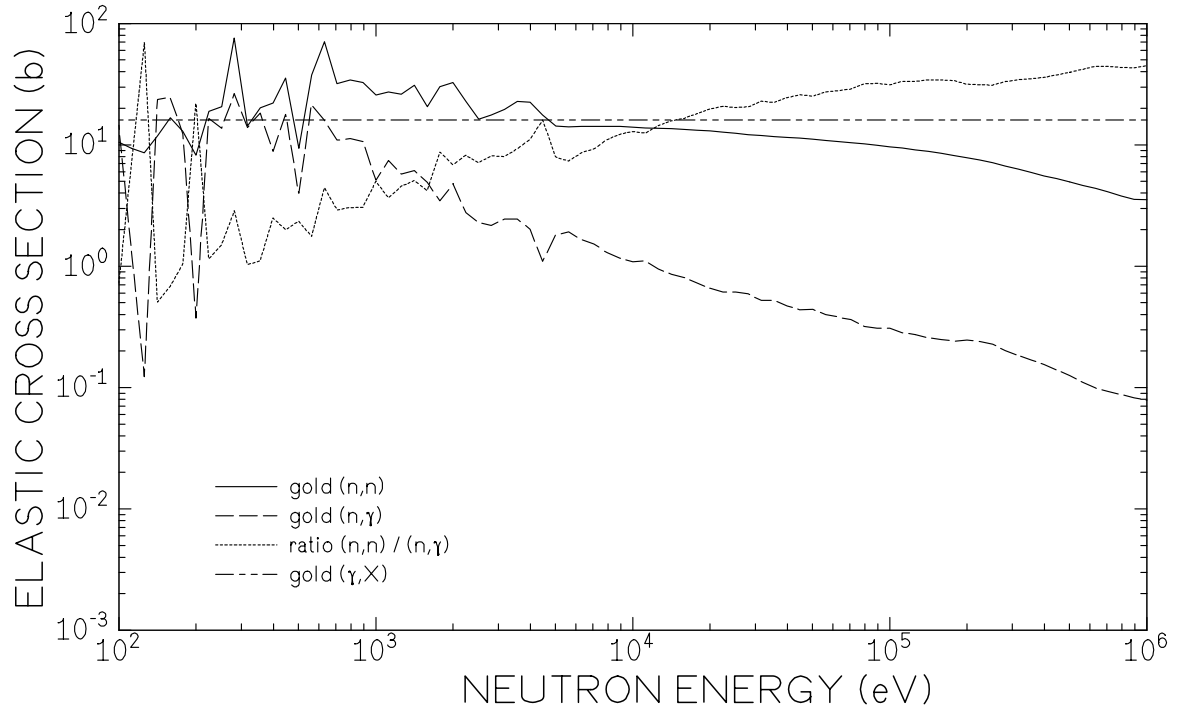


**Figure 2:** Comparison of (n,X) and (γ,X) cross sections for gold.

### 3 Determination of (n,n) and γ-induced background

#### 3.1 Cross sections

Table 1 contains a summary of neutron scattering cross sections as well as total cross section for 10 MeV γ-rays. Experiments and FLUKA simulations at n-TOF as well as GEANT and MCNP simulations for target 1 at WNR show that about 1 γ-ray per 10 neutrons will be present at the sample position in the keV-neutron TOF region. Taking into account that the detection efficiency for photons is about 100%, while it is only 10% for neutrons, this means that the ratio between events caused by scattered neutrons to events due to scattered photons is *equal* in relation to the respective interaction cross section of the isotope at the sample position.

**Table 1:** Summary of the neutron scattering cross sections for keV-neutrons and total reaction cross section for 10 MeV γ-rays of different isotopes.

Isotope	(n,n)	$E_{\min}$	$E_{\max}$	$(\gamma,x)$ ( $E_\gamma = 10$ MeV)	$(n,n) / (\gamma,X)$
nat. Pb	10 b	1 meV	10 MeV	20 b	< 0.5
nat. Ti	1 .. 100 b	10 keV	100 keV	2 b	0.5 .. 50
<b><math>^{32}\text{S}</math></b>	<b>0.02 .. 20 b</b>	<b>70 keV</b>	<b>100 keV</b>	<b>1.5 b</b>	<b>.013 .. 13</b>
nat. C	5 b	10 meV	10 MeV	0.3 b	< 17
nat. Be	6 b	10 meV	10 MeV	0.3 b	< 20
D	3.5 b	0.1 eV	1 MeV	0.05 b	< 70
H	20 b	1 keV	0.1 MeV	0.05 b	< 400

The  $\gamma$ -ray spectrum depends strongly on the reaction causing the photons as well as on the specific setup. The  $\gamma$ -spectrum at late times (long time of flight) consists mainly of two components:

- prompt photons due to capture of moderated neutrons
- photons due to the decay of (neutron induced) reaction products

The component due to the decay of reaction products was measured at FP14 3 months after the shutdown of the accelerator (Figure 3). All the lines which can be seen there correspond to activation due to neutron induced reactions on aluminum alloy and stainless steel. Both materials are present in windows upstream of the shutter. Especially the water moderator, which is exposed to the highest neutron flux, consists of water in a aluminum alloy housing.

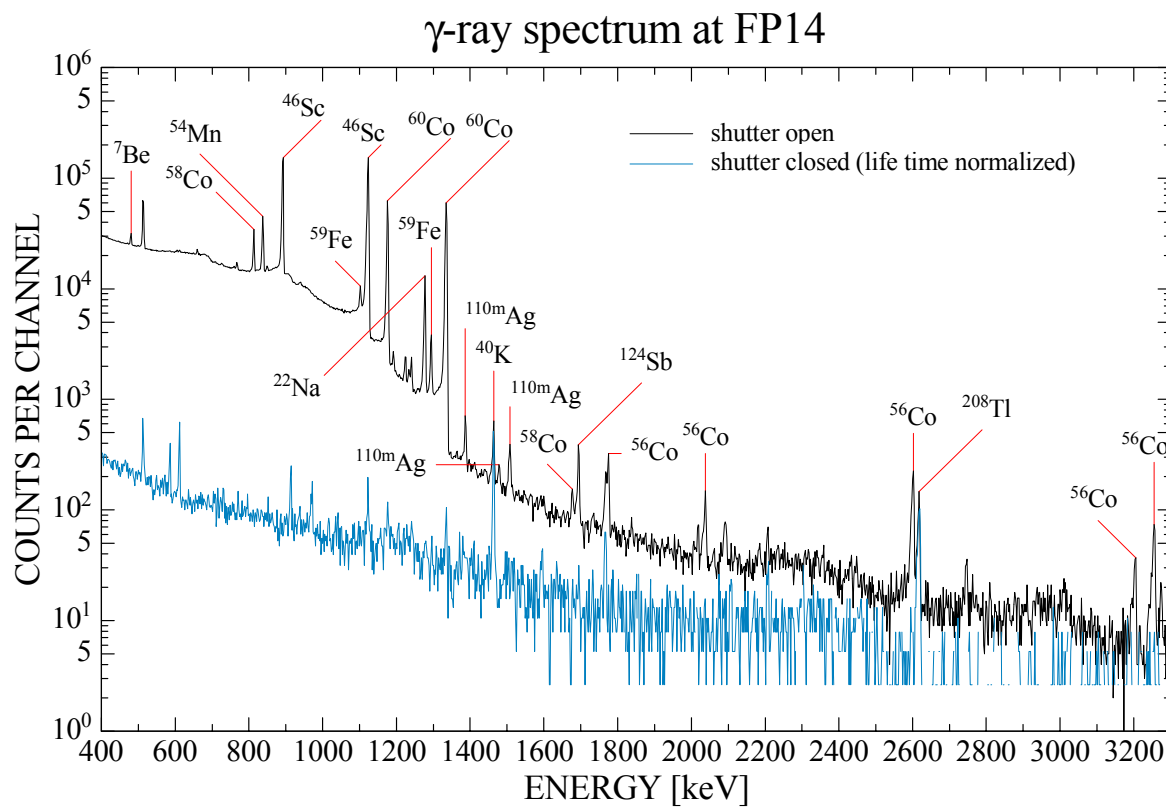


**Figure 3:** Photon activity measured at FP14 at april-17 2003, 3 month after the shut down of the accelerator.

In order to confirm this observation, an additional measurement shortly after a beam shutdown would be very helpful and is planned for the future.

The capture  $\gamma$ -ray component has not been measured yet. Since the neutron as well as the gamma flux during the operation is very high, it is almost impossible to place any kind of detector directly in the beam. Indirect methods need to be applied.

The neutron scattering to photon interaction ratio of sulfur changes between 70 and 100 keV over 2 orders of magnitude (Table 1 and Figure 4). Therefore the ratio of  $\gamma$ -rays to neutrons could be determined using a sulfur sample in the DANCE ball and applying TOF-cuts. At the top of the scattering resonance ( $\sim 100$  keV) the signal in the BaF<sub>2</sub> array will be dominated by scattered neutrons, which will be captured after moderating. At time of flights corresponding



to the low energetic tail of the resonance around 70 keV however, the count rate will be dominated by interactions of photons with the sample. Neutron capture at the sample has a very low cross section and can almost be neglected.

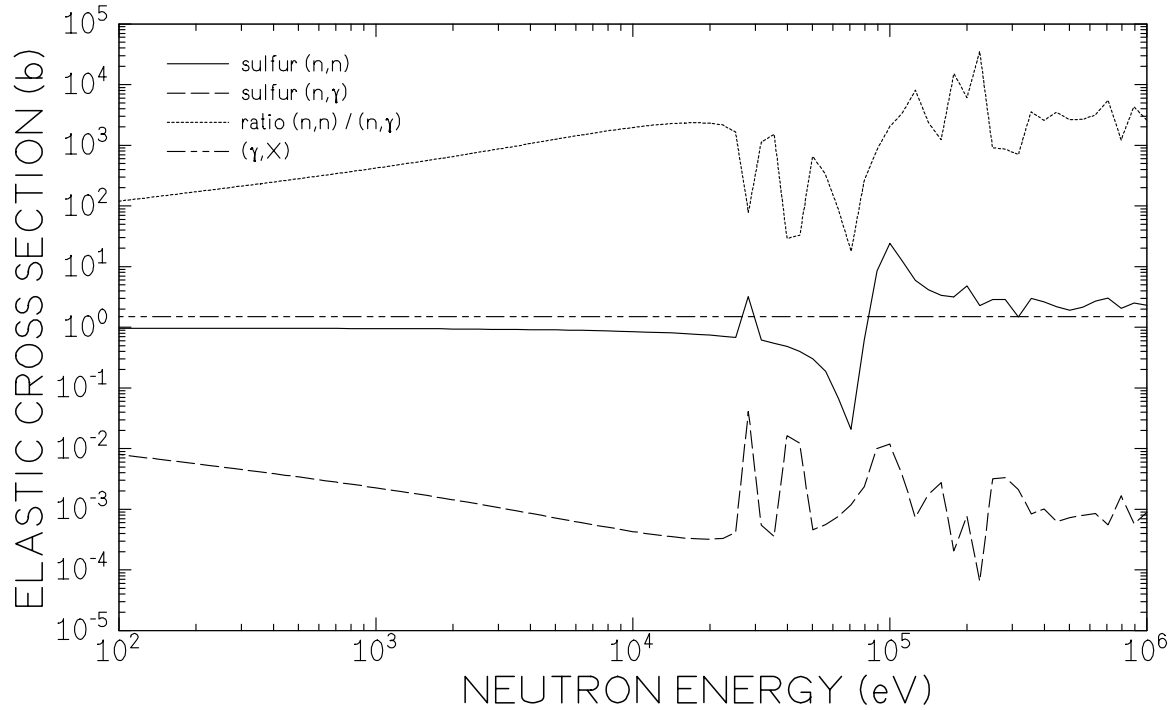


**Figure 4:** Comparison of  $(n,X)$  and  $(\gamma,X)$  cross sections for sulfur.

The scattered neutrons will not be captured instantaneously. Most of the captured neutrons will be moderated in the  $\text{BaF}_2$  crystals before the actual capture occurs. The described method works only, if this time is small compared to the difference in time of flight for a 100 keV and a 70 keV neutron, which is  $0.9 \mu\text{s}$  for 20.25 m flight path.

For most of the other isotopes this ratio doesn't change as much as for sulfur within a short neutron interval. For the typical scatter samples carbon and lead it is almost constant over a broad energy range (see Figure 5 .. Figure 7). In the next chapter the response of the DANCE array has therefore been investigated for different isotopes, trying to find a possibility of using different samples in the crystals ball in order to disentangle the different background components.

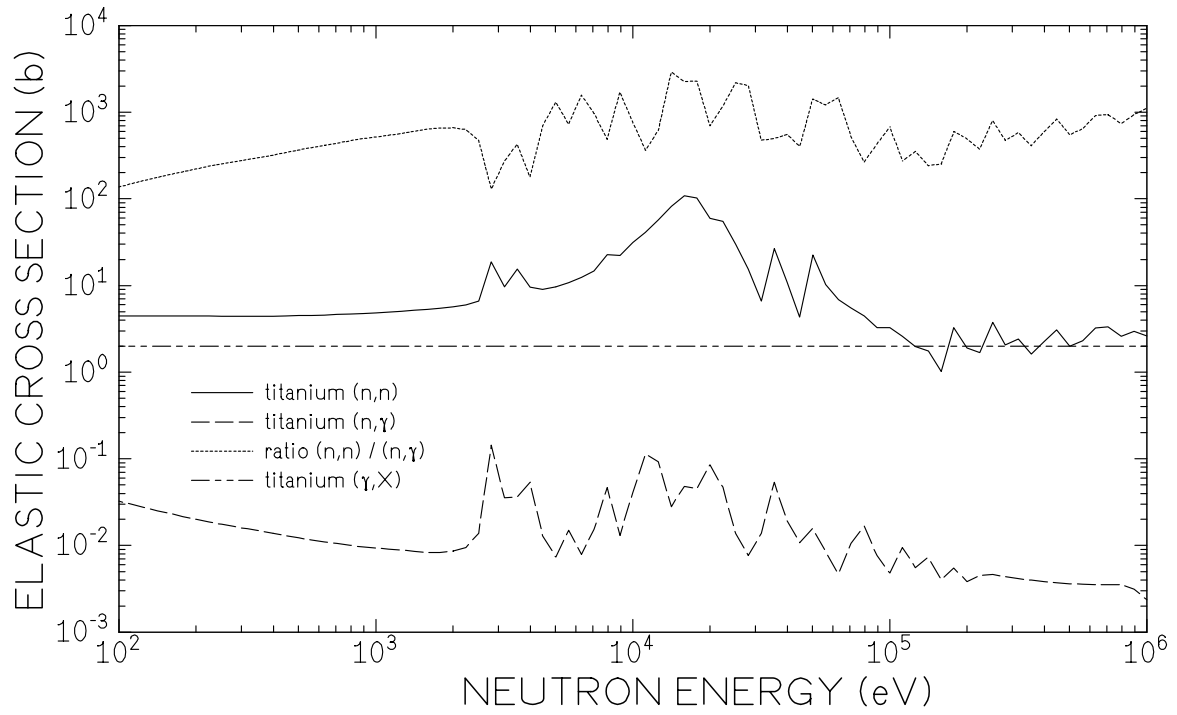


**Figure 5:** Comparison of (n,X) and (γ,X) cross sections for titanium.

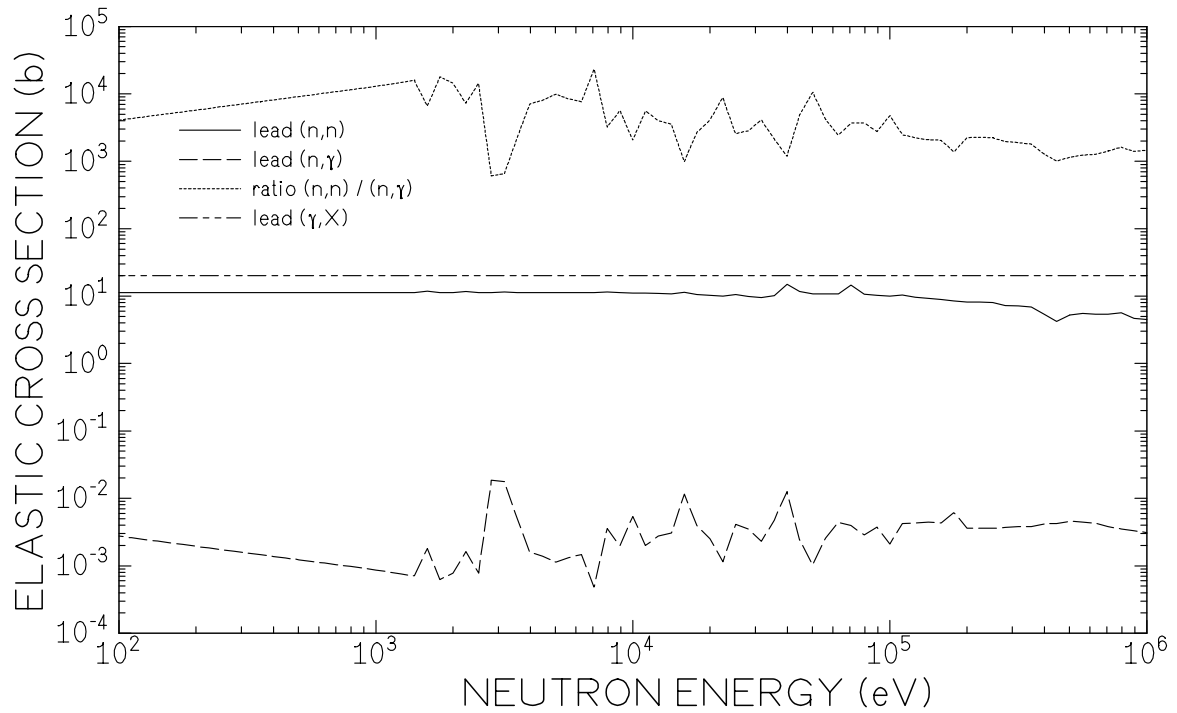


**Figure 6:** Comparison of (n,X) and (γ,X) cross sections for lead.

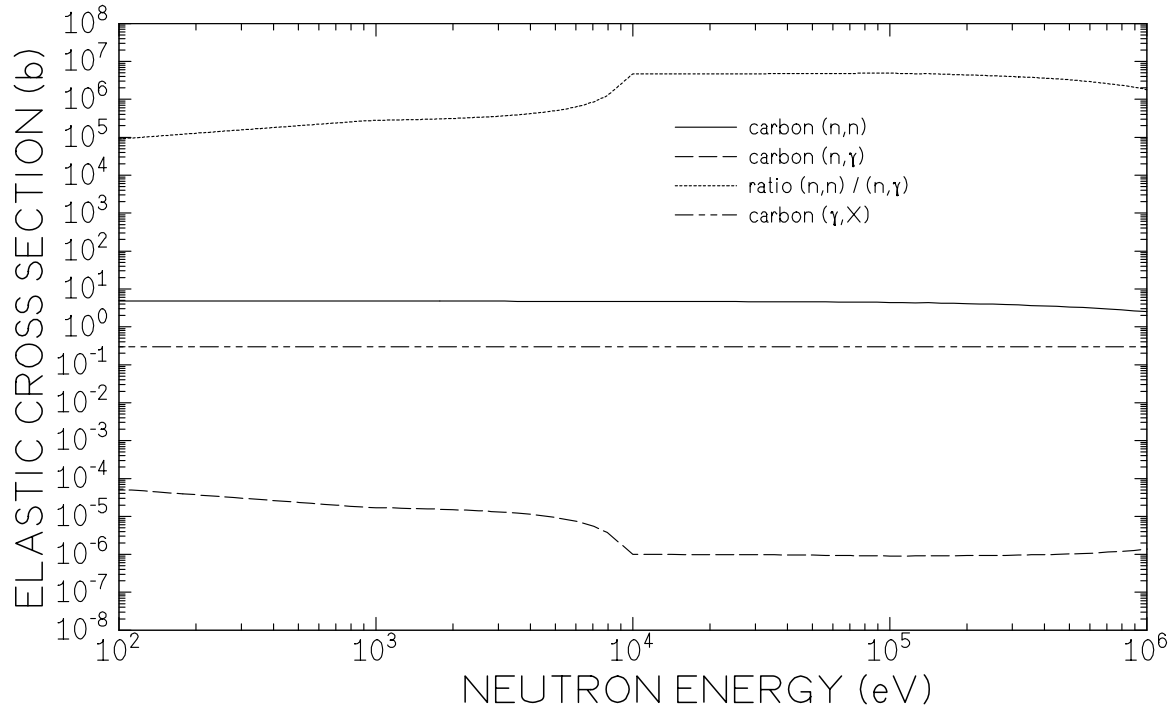


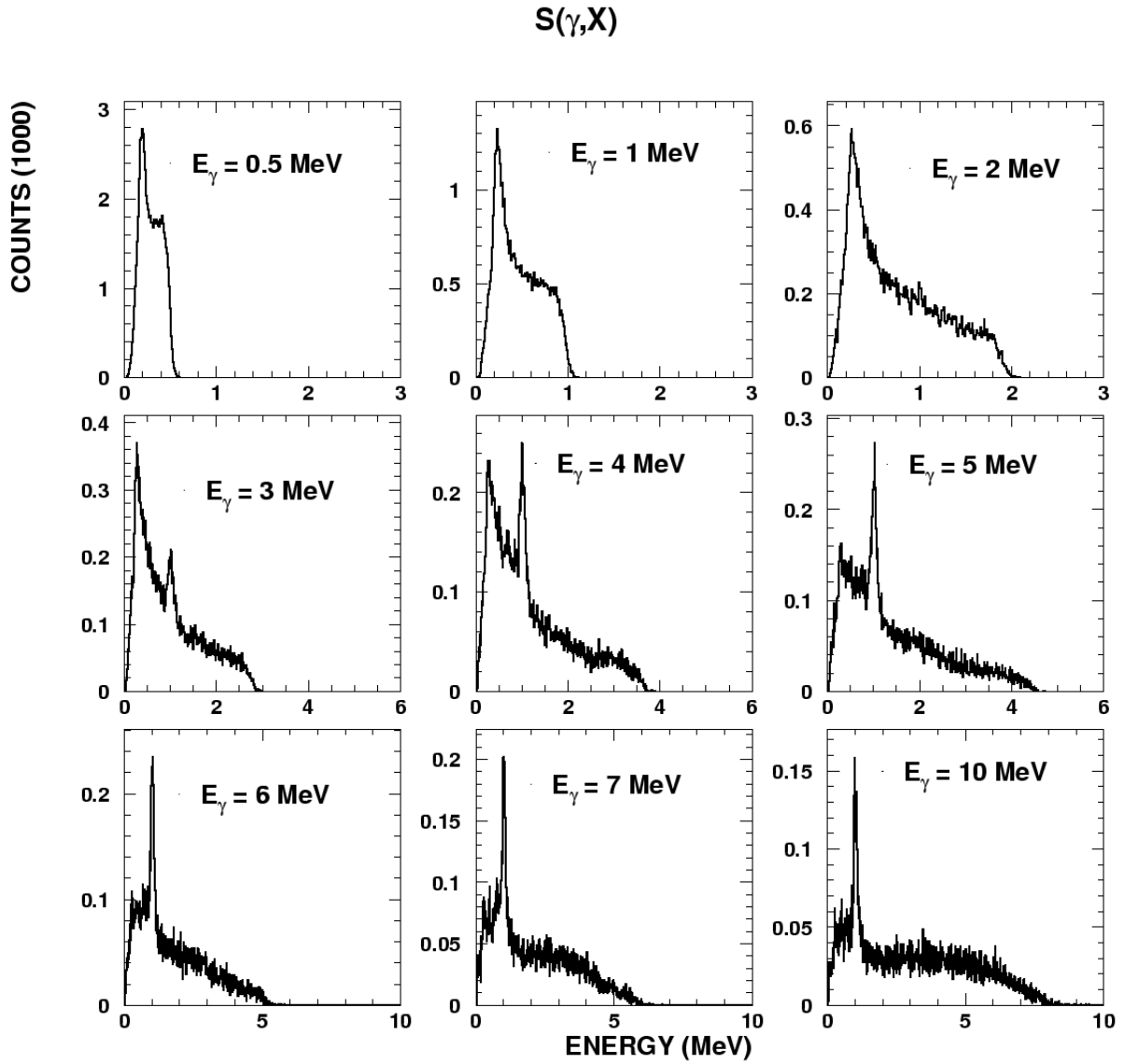
**Figure 7:** Comparison of (n,X) and (γ,X) cross sections for carbon.

### 3.2 Detector response

The following figures are representing the results of simulations carried out with GEANT 3.21. The response of the DANCE (cite earlier report) BaF<sub>2</sub> array with 160 crystals and no single detector threshold has been simulated. The simulations have been carried out for different samples with gammas and neutrons of different energies. The neutron energy range shown in the figures corresponds to 1 .. 100 keV with a 1/E spallation spectrum. The first figure of each isotope shows the response to γ-rays of different energies coming along the neutron beam pipe and interacting with the respective sample. The second figure shows a comparison of photon to neutron interactions with the sample. The gamma spectrum assumed was a unweighted sum of 0.5, 1, 2, 3, 4, 5, 6, and 7 MeV. The total number of photons corresponds to 1/10 of the number of neutrons.

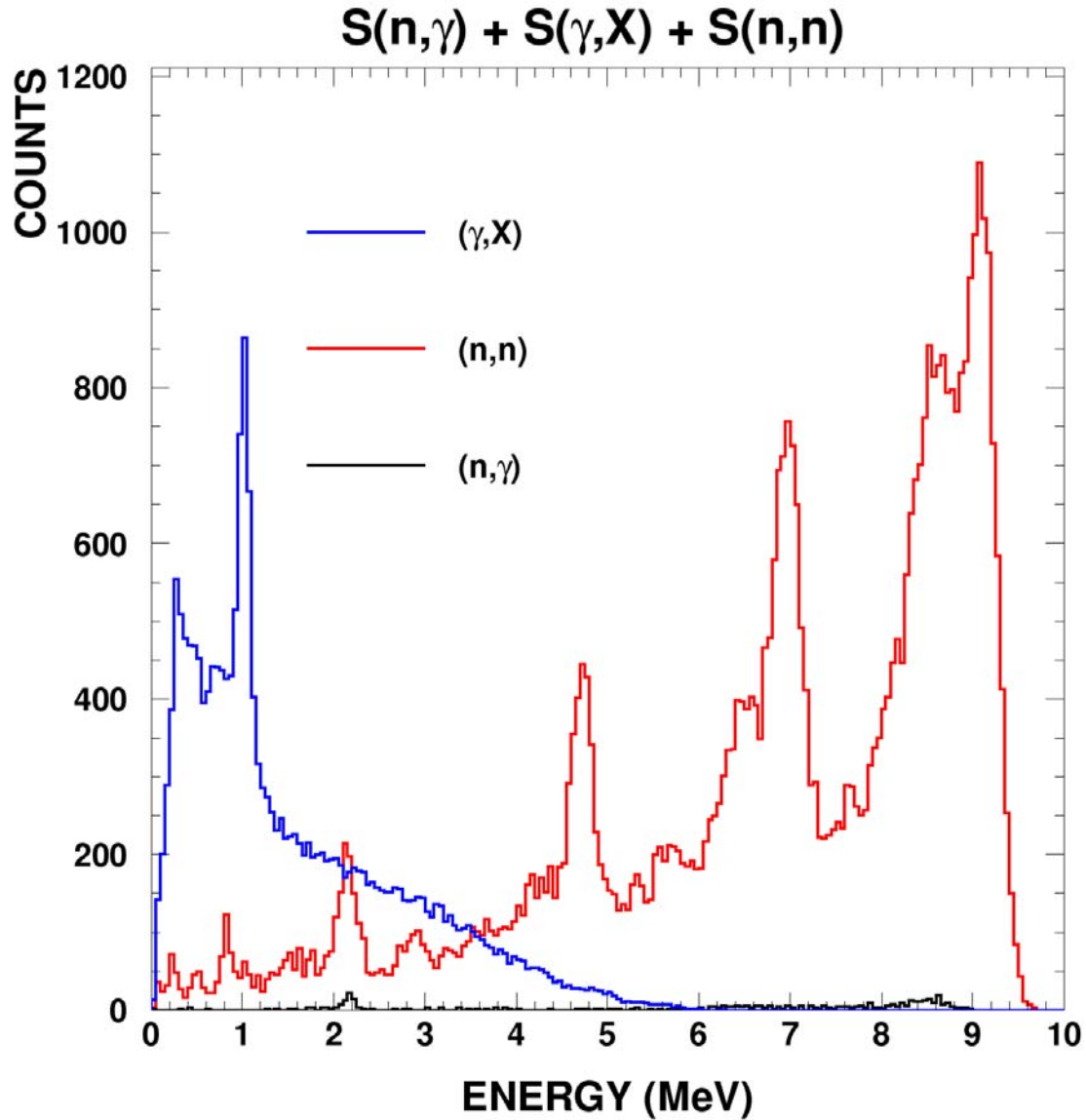
The cylindrical samples had always a diameter of 1 cm and different thicknesses. The thicknesses had been chosen in order to gain enough statistics with a constant number of simulated neutrons and gammas.

Figure 8 and Figure 9 show the results for 5 mm sulfur sample. High energetic photons interact primarily due to pair production. This leads to a remarkable peak at 1.02 MeV in the  $\gamma$ -ray spectrum (Figure 8).



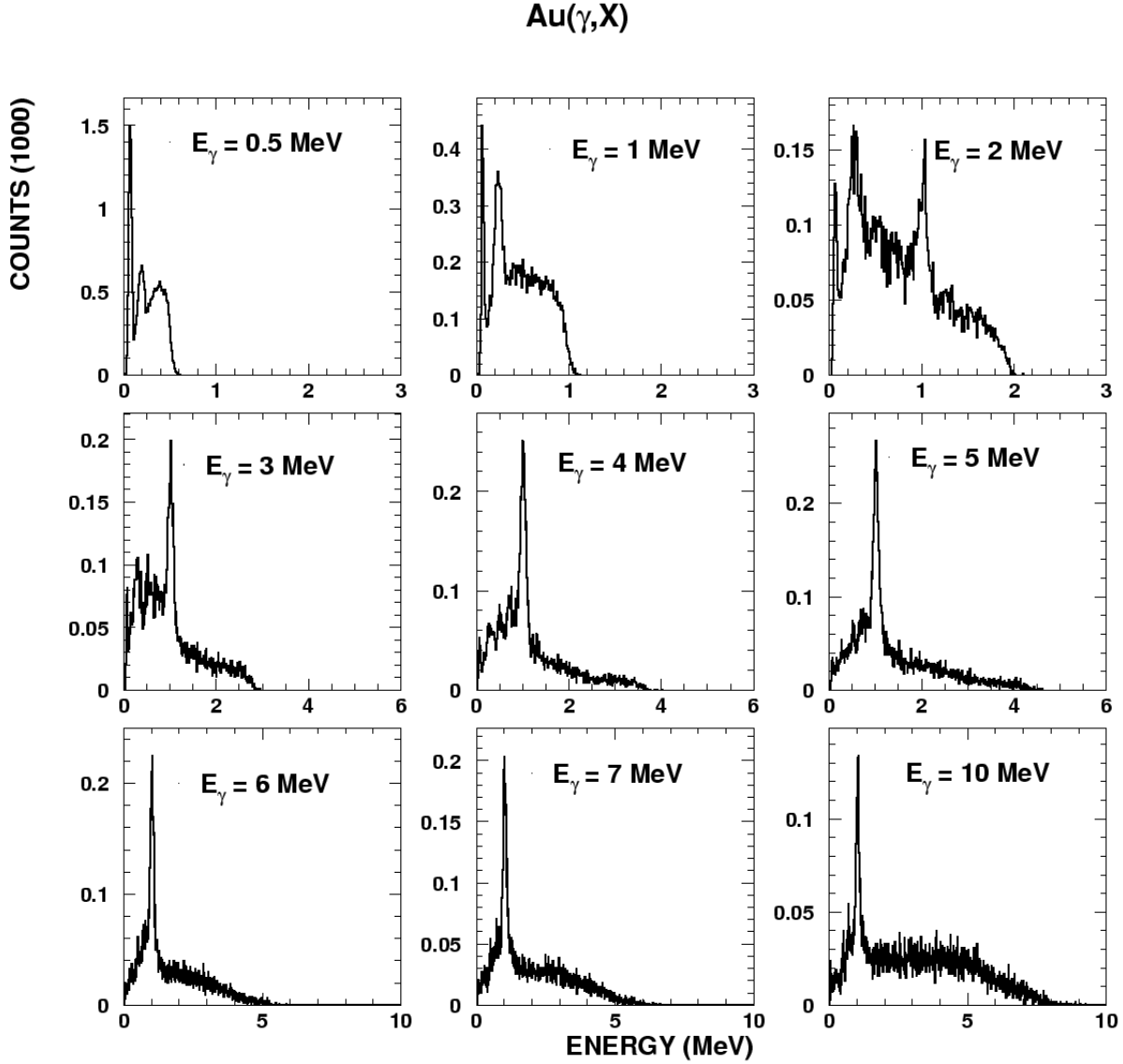
**Figure 8:** Response of the BaF<sub>2</sub>-array to g-rays of different energies interacting with a sulfur sample (5 mm thickness) in the center of the detector.

Compared to the events due to neutron reactions, the  $\gamma$ -ray events are dominating below 2 MeV, while neutrons are dominating above 4 MeV (Figure 9). Neutron capture events can not be observed, when all the other components are present as expected. Since Figure 9 corresponds to averaged neutron energies, the background determination method described in the previous chapter – using a sulfur sample in the center of the  $\text{BaF}_2$  ball with TOF cuts – seems to be promising. Both background components are present and of the same order.



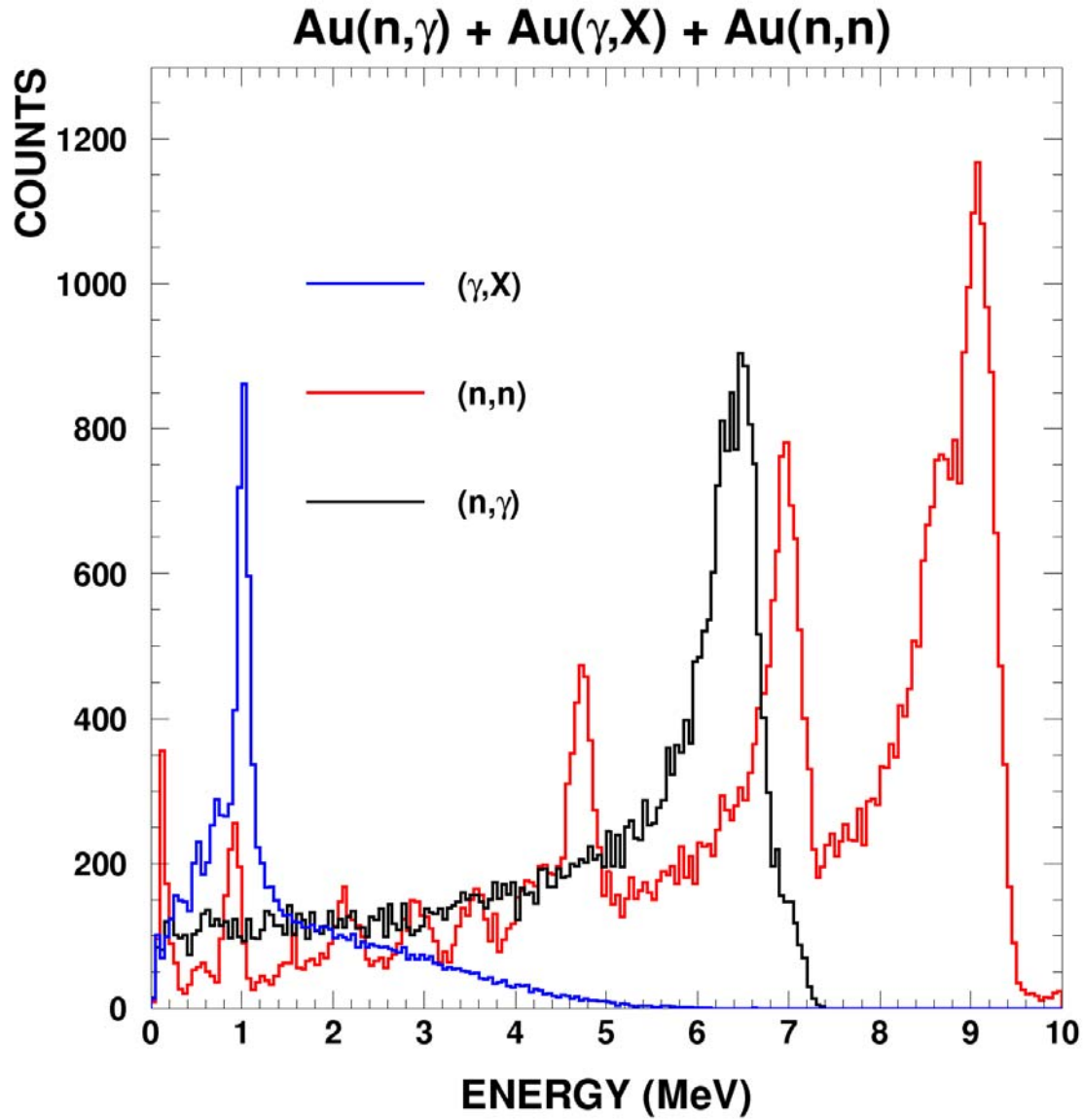
**Figure 9:** Comparison  $S(n,\gamma)$  (black)  $S(\gamma,X)$  (blue) and  $S(n,X)$  (red).

Gold is the most important reference for neutron capture measurements in the keV region and most of the experiments carried out at DANCE will be relative to gold. Therefore it is crucial to understand every component of the signal seen in the detector with a gold sample in place. Figure 10 and Figure 11 show the results of the respective simulations for a 0.2 mm gold sample. Compared to the  $\gamma$ -ray spectra shown for sulfur, the pair production dominates already at smaller photon energies. This observation reflects the increasing pair production cross section with increasing atomic number (Figure 10).



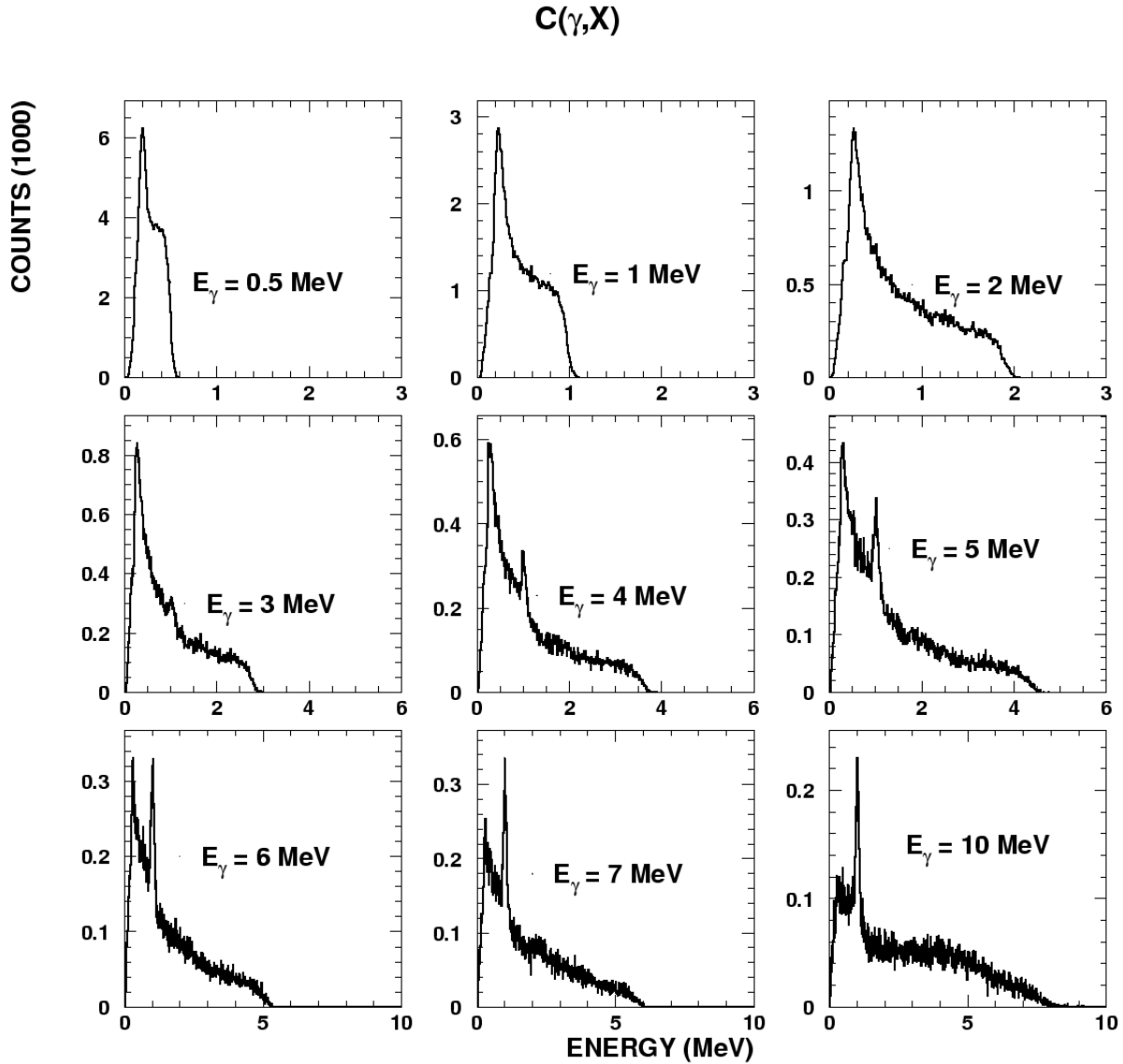
**Figure 10:** Response of the BaF<sub>2</sub>-array to g-rays of different energies interacting with a gold sample (0.2 mm thickness) in the center of the detector.

The neutron capture as well as neutron scattering cross sections of gold are comparably huge. Therefore neutron induced events are dominating the total energy spectrum above 2 MeV, while only at energies below 1.5 MeV, especially around the strong 1.02 MeV peak, events due to photon interaction with the sample are dominating the spectrum (Figure 11). Depending on the energy, the neutron induced events are either due to neutron capture or neutron scatter.



**Figure 11:** Comparison Au(n, $\gamma$ ) (black) Au( $\gamma$ ,X) (blue) and Au(n,X) (red).

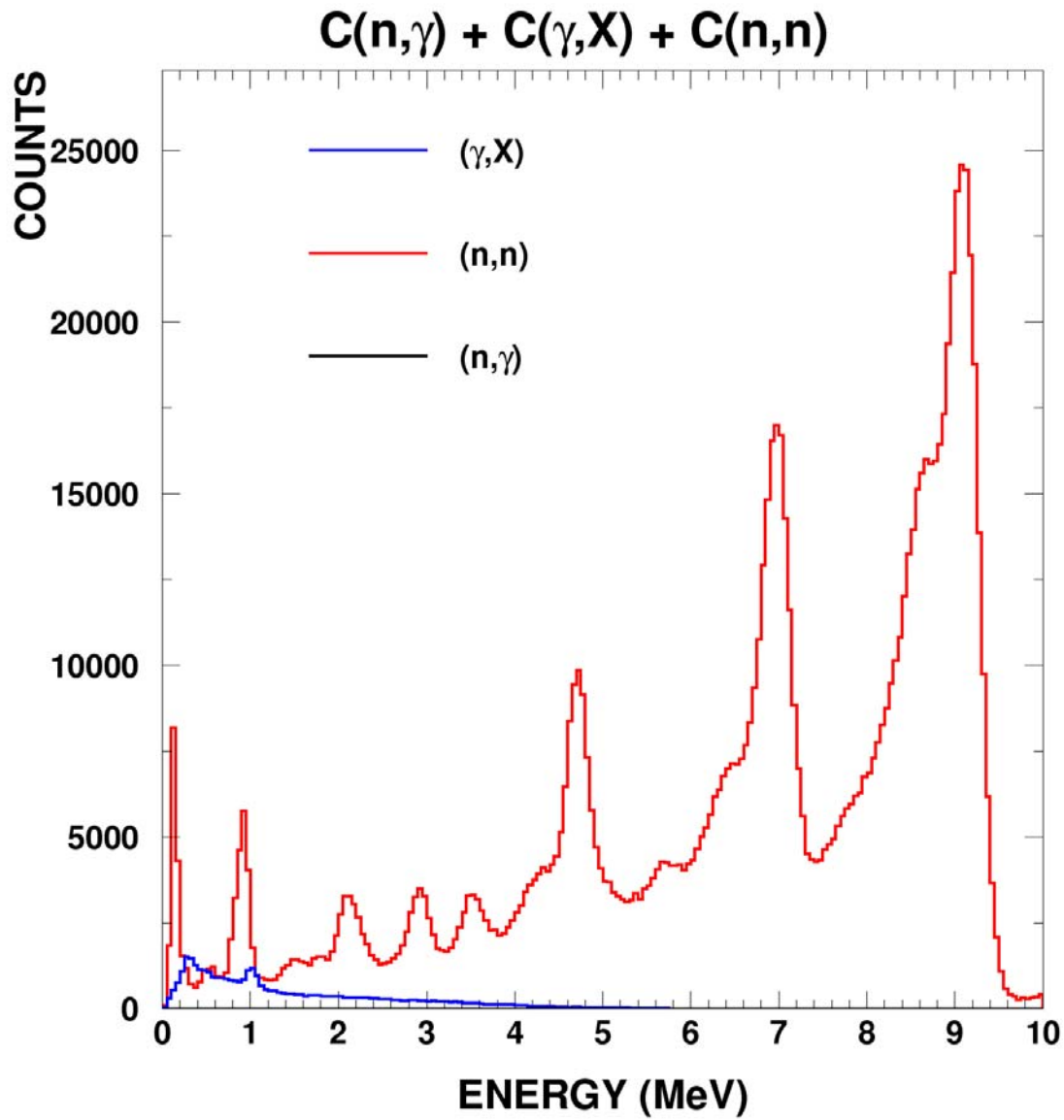
Carbon is often used for determining the neutron scattering background, since the neutron capture cross section is orders of magnitude smaller than the scattering cross section. Figure 12 shows a typical response to photons on a sample with low atomic number. The most important interaction mechanisms are photo effect and Compton scattering. Therefore, the 1.02 MeV peak due to pair production can only be observed for primary photons above 4 MeV.



**Figure 12:** Response of the BaF<sub>2</sub>-array to g-rays of different energies interacting with a carbon sample (10 mm thickness) in the center of the detector.

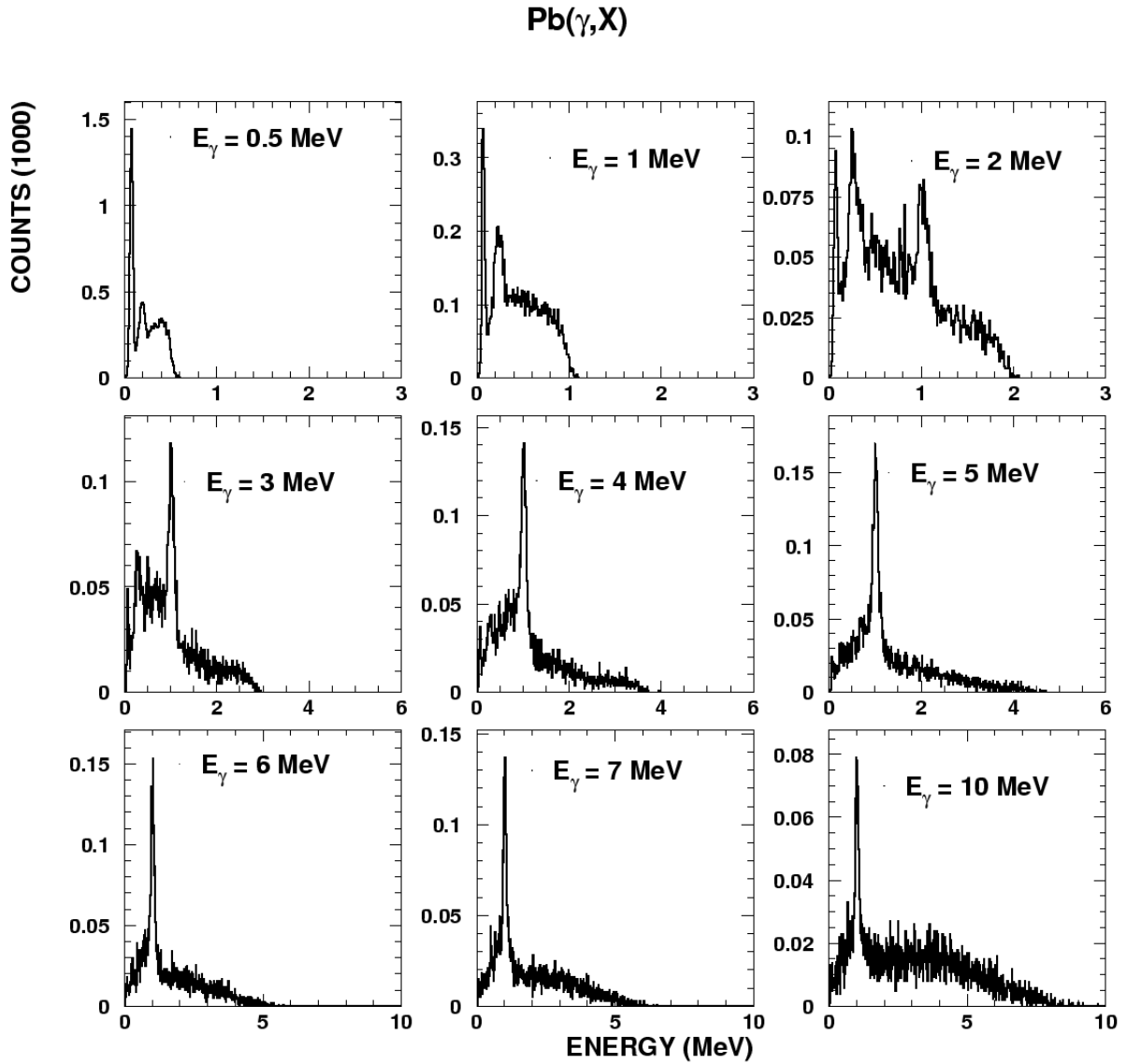


According to Figure 13 neutron induced events are dominating the spectrum over the whole energy range. Only at the lowest energies (below 1.5 MeV) events due to photon interaction are of the same order of magnitude. Neutron capture on carbon doesn't contribute at all.



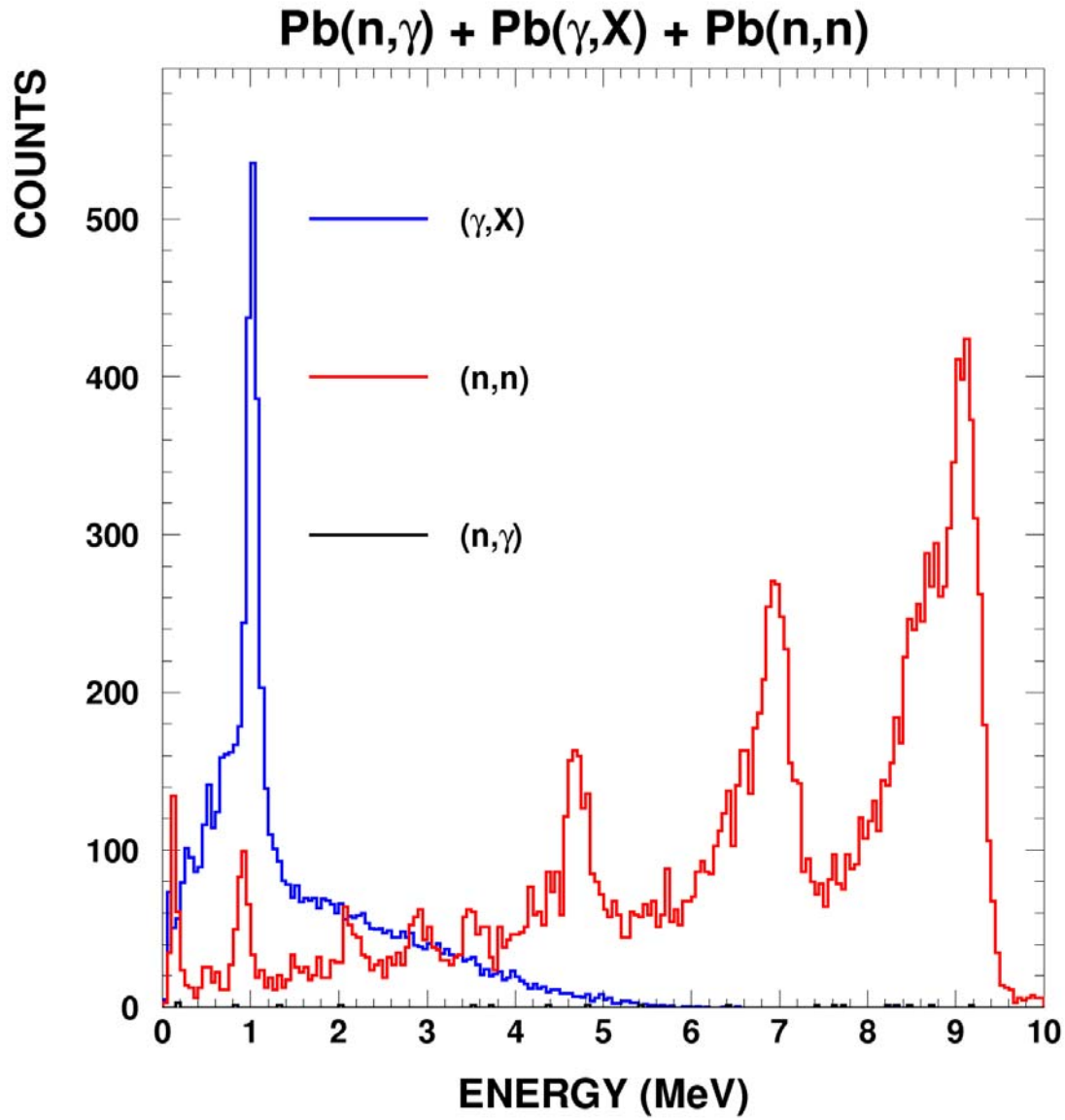
**Figure 13:** Comparison  $C(n,\gamma)$  (black)  $C(\gamma,X)$  (blue) and  $C(n,X)$  (red).

Another important neutron scattering sample is lead. In contrast to carbon, lead shows the spectra for photon interaction with heavy nuclei (Figure 14). The most important interaction is pair production, resulting in a 1.02 for all photons above the production threshold.



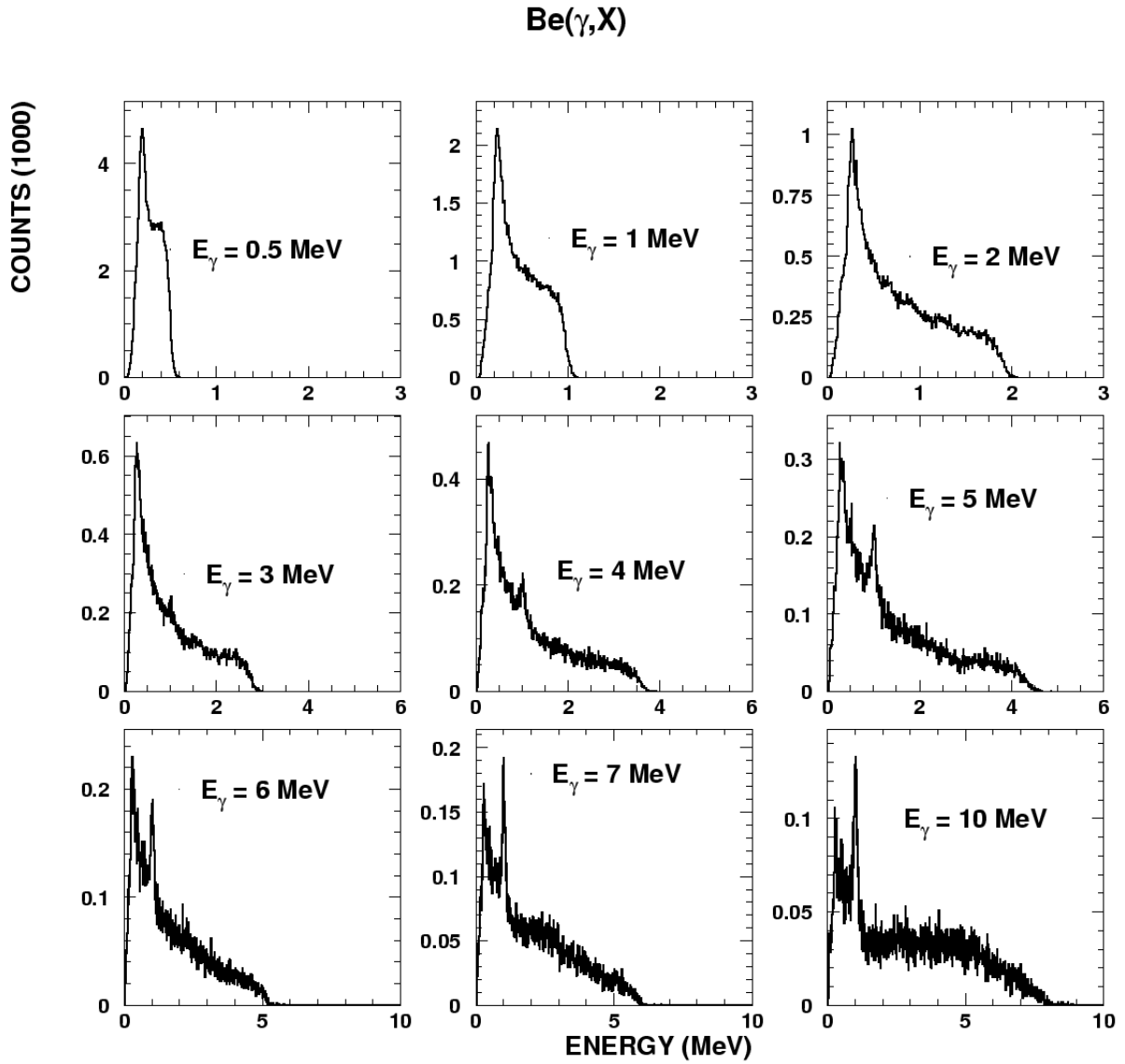
**Figure 14:** Response of the BaF<sub>2</sub>-array to g-rays of different energies interacting with a lead sample (0.2 mm thickness) in the center of the detector.

Figure 15 shows that photon induced events contribute significantly below 3 MeV and are dominating the spectrum below 2 MeV. Neutron capture doesn't play any role at all. Therefore a comparison of the experimental data of carbon and lead would give immediate hints on the relative numbers of gammas to neutrons in the beam.



**Figure 15:** Comparison  $\text{Pb}(n,\gamma)$  (black)  $\text{Pb}(\gamma,X)$  (blue) and  $\text{Pb}(n,X)$  (red).

Many samples for experiments at DANCE will be mounted on beryllium backings. The response to different beam components of this backing is therefore of interest. Figure 16 shows the response to  $\gamma$ -rays.



**Figure 16:** Response of the BaF<sub>2</sub>-array to  $\gamma$ -rays of different energies interacting with a beryllium sample (10 mm thickness) in the center of the detector.

The comparison presented in Figure 17 looks very similar to the carbon. Neutron scattering events are dominating the background over the whole energy range.

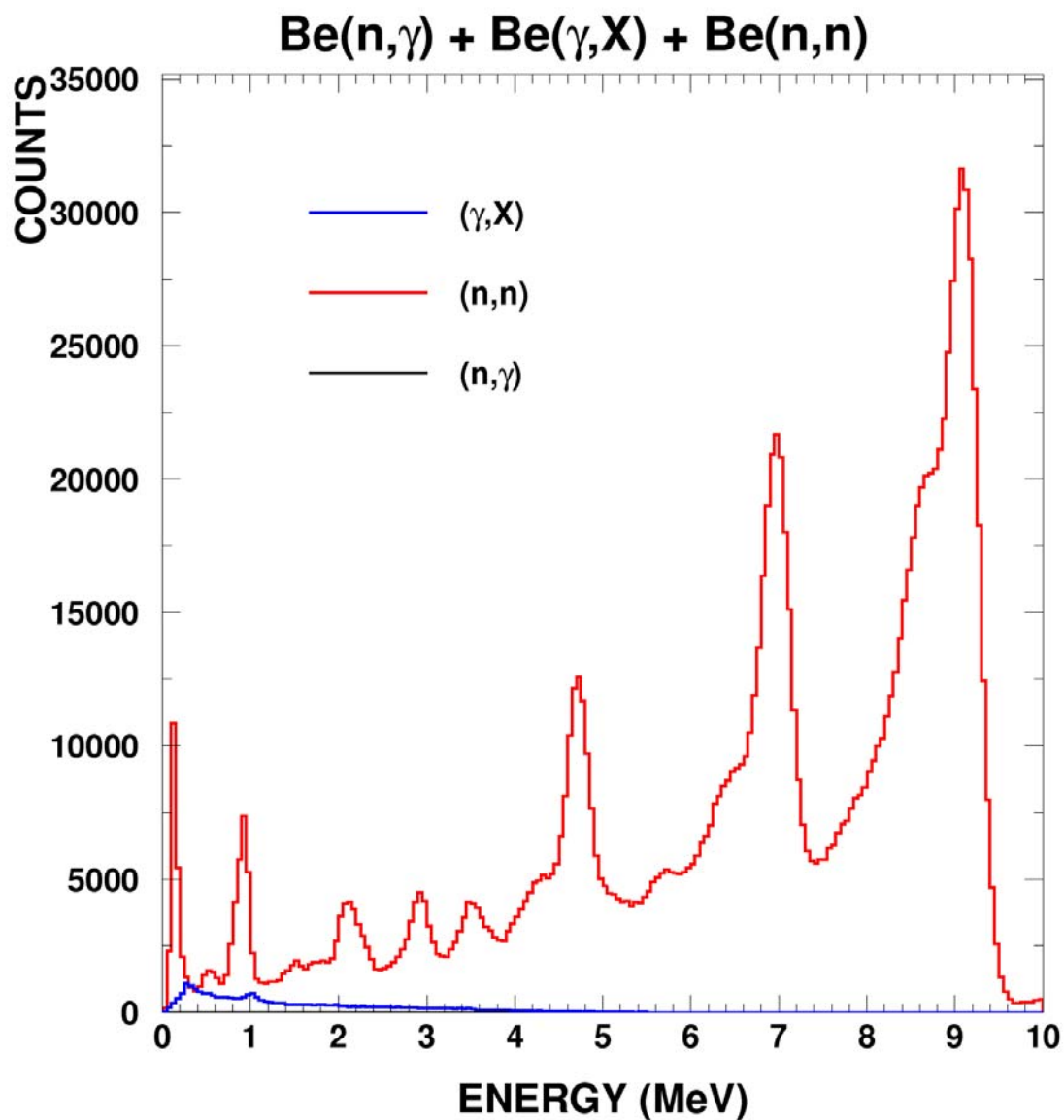


**Figure 17:** Comparison Be(n,γ) (black) Be(γ,X) (blue) and Be(n,X) (red).

## 4 Conclusions

The simulations reported here as well as experiences at other experiments imply that the background caused by late  $\gamma$ -rays – arriving at the sample at the same time as the neutrons – is an important component for neutron capture experiments and cannot be neglected, especially for heavy elements. In order to characterize this background component during an experiment it is not only necessary to know the absolute number of photons, but also their energy distribution.

A piece of polyethylene (PE) with 1.4 cm thickness upstream of the sample reduces the neutron flux at the sample below 100 keV by at least a factor of 10, while the  $\gamma$ -ray flux is not reduced by more than 5 %. Together with the different response to different isotopes most of the information needed for determining the  $\gamma$ -ray spectra – as a function of TOF ! – can be gained by the following measurement campaign:

- determining the activation spectrum as short as possible after a beam shutdown using germanium detectors
- determining the additional prompt component with a  $4\pi$ -detector and 4 different setups:
  - carbon sample
  - carbon sample and 1.4 cm PE
  - lead sample
  - lead sample and 1.4 cm PE
- if the flight path is sufficiently long (at least 20 m) an additional measurement using a sulfur sample (with and without PE) gives even more valuable information.

## References

1. Koehler P.E., *Nucl. Instr. Meth. A* **460** (2001) 352 .
2. Bockhoff K.H., et al., *Nucl. Sci. Eng.* **106** (1990) 192.
3. Corvi F., Mutti P., Zanini L., *Dokladi-Biad* **5** (2000) 41.
4. Mutti P., et al., *Nucl. Phys.* **A621** (1997) 262c .
5. Abramovich S., et al., *CERN Report*, **CERN/SPSC 99-8; SPSC/P 310** (1999).
6. Lisowski P.W., et al., *Nucl. Sci. Engineering* **106** (1990) 208.
7. XCOM: X-ray Attenuation Databases,  
[www.physics.nist.gov/PhysRefData/Xcom/Text/XCOM.html](http://www.physics.nist.gov/PhysRefData/Xcom/Text/XCOM.html), NIST (2002).